Chapter 11

Investigation of Bioluminescence at an Optical Fiber End for a High-Sensitive ATP Detection System

Masataka Iinuma, Ryuta Tanaka, Eriko Takahama, Takeshi Ikeda, Yutaka Kadoya and Akio Kuroda

Additional information is available at the end of the chapter

http://dx.doi.org/10.5772/52747

1. Introduction

In biological research, the luminescience from fluorescent proteins or luminescent enzymes is widely applied for monitoring a change of environment at a cell. Biomolecules used as the probe, such as Green Fluorescence Protein (GFP) or luciferase molecules found in fireflies can respond to the existence of specific molecules or ions and subsequently emit a photon. The detection of a specific molecule can then be confirmed by detecting the emitted photons efficiently with a photon detector. A highly efficient detection of the luminescence is normally essential to realization of a high sensitivity to the specific molecules or ions and an improvement of the sensitivity can upgrade the capability of detection in a low concentration of sample solution. Therefore, there are many efforts to improve the efficiency of the collection of emitted photons and of the optical coupling to the photon detector.

A straightforward method is to directly detect the luminescence from the sample solution in a test tube with a single photon detector via simple coupling optics as shown in Fig. 1. This detection system is very simple and easy-operational, so that it has been widely used for various applications so far. To realize high efficiency detection, however, this method needs a single photon detector with the wide photon-sensitive area, which is ideally larger than a photon-emission area in the test tube. Here, we are introducing an alternative method, where the luminescent biomolecules are immobilized at an optical fiber end and the luminescence is detected by a photon detector which is optically coupled to the other optical fiber end. Fig. 2 illustrates the optical fiber-based system. This method has been investigated for application to a fiberoptic biosensor, which is constructed by immobilizing either an enzyme or an antibody. A review of this method is given in reference [1] and [2].

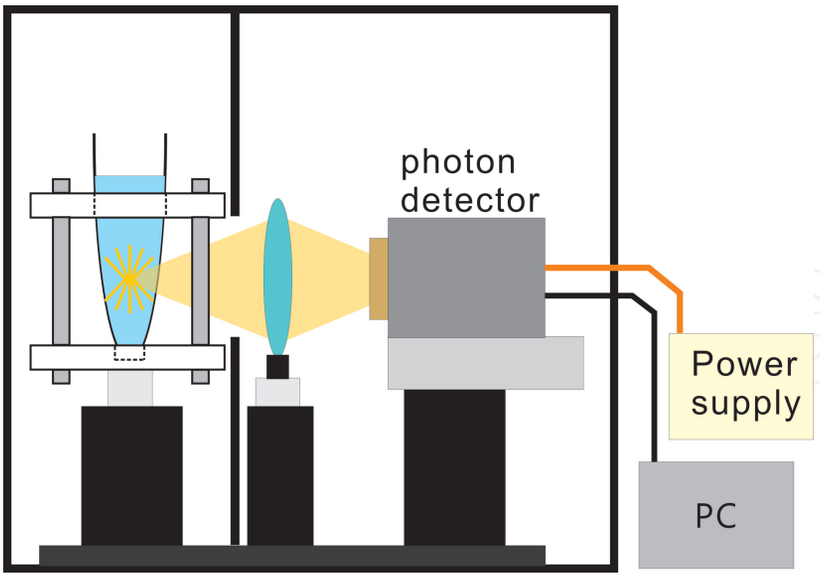

Figure 1. Direct detection system of luminescence

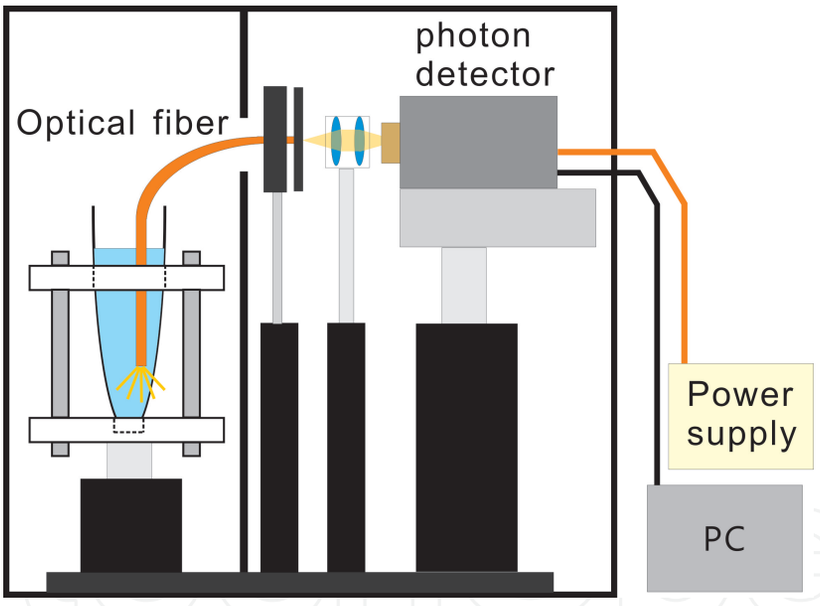

Figure 2. Optical fiber-based system of luminescence

This method has three merits. The first one is to permit a local detection within the sample solution, because the optical fiber end functions as a needle-like probe. Meanwhile, the method as shown in Fig. 1 is suitable for detecting the luminescence from a large area in the sample solution. The second one is that the detection scheme does not require that the photon detection is very close to the sample solution. This feature makes it easier to mount the sensing parts in integrated bioengineering, such as μ -TAS. The third merit is that single photon detectors with a small sensitive area are also available, because the photon-emission area, which is almost identical to the cross section of the core part in the optical fiber, is small. In general, single

http://dx.doi.org/10.5772/52747

photon detectors have lower dark counts for smaller sensitive area. Low noise is very important, because it essentially gives the upper limit of the sensitivity of photon detection. Recently, single photon detectors using avalanche photo diodes (APDs) have become widely available with good performance, but their sensitive area is small and typically 0.1 mm. The luminescence detection with the optical-fiber based system allows us to fully use the merits of compactness, high quantum efficiency, and low noise of these APD detectors. On the other hand, single photon detectors using compact and cooled photomultiplier tubes (PMTs) are also available, since they have the characteristics of low noise and much larger sensitive area than the APD's. Moreover, their quantum efficiency is not so much lower than the APD's. The fiber-based system with these PMT detectors can make a fully use of the merits of large sensitive area and low noise of the PMTs, although the quantum efficiency is lower than the APD's.

We have built detection systems of bioluminescence at an optical fiber end and investigated the sensitivity of Adenosine triphosphate (ATP) detections by using an APD-type as described in [3] and [4]. In this chapter, results with a PMT-type detector are presented in comparison with the results by using the APD-type photon detector. We also discuss the reason of limiting the present sensitivity in the system with the PMT-type detector. ATP is a good indicator of biochemical reaction or life activity, since ATP is considered as the universal currency of biological energy for all living things. Therefore, there are many efforts to develop ATP-sensing techniques for compact and efficient ATP detection in reference [5-7]. In particular, high-sensitivity detection of ATP can indicate the existence of microorganisms even in low numbers. Thus, a compact, simple, and easy-operational system with extremely high sensitivity has been desirable.

One well-known and powerful method for highly sensitive ATP detection is to use the chemical reaction involved in thebioluminescence, the luciferin-luciferase reaction in reference [8]. In this reaction, after one ATP molecule and one luciferin molecule are bound to one luciferase molecule, and the luciferin molecule is oxidized using the energy of ATP. As consequence, one photon is emitted during the transition from the excited state to the ground state of the oxidized luciferin molecule bound to the luciferase molecule. The emission of one photon indicates the use of the energy of one ATP molecule. In the method using the luciferin-luciferase reaction, the efficient detection of the bioluminescence is essential for high-sensitivity detection of ATP.

The oxidation of luciferin is catalysed by the enzyme luciferase, so that the immobilization of luciferase molecules on solid probes of various sizes allows highly sensitive and local detection of ATP. Three types of immobilization have been used: firstly attachment to the cell surface in [9], secondary attachment to small particles, such as nanoparticles in [10], glass beads and rods in [11], thirdly attachment to extended objects with a size in the centimeter range, such as strips in [12] and [13], and films in [14]. For the ATP-detection on the intermediate scale below 1 millimeter, a fiberoptic probe employing immobilized luciferase in [2] as well as microchips in [15] and [16] is utilizable. Therefore, the efficient detection system of bioluminescence at an optical fiber end can achieve the local detection of ATP. The realization of highly sensitive detection of ATP potentically provides the local detection of extremely low number of microorganisms. Thus, it is desirable to construct a highly efficient detection system of the

bioluminescence at an optical fiber end and to evaluate the detection limit with the system. In order to explore possibilities for improving the detection limit, moreover, it is also necessary to investigate the bioluminescent reaction at an optical fiber end.

The rest of this chapter is organized as follows. In sec. 2, we describe a concept for the construction of the optical fiber-based system and show how to construct the detection systems by using the PMT detector. In sec. 3, we describe the sensitivity test with the constructed system and show the results are consisitent with the APD, but also show that the sensitivity can not reach the expected detection limit. In sec. 4, we present the results of kinetic properties obtained from experimental data on the bioluminescence and clarify a dominant reason of restricting the detection limit.Sec. 5 summarizes prensent results and future problems.

2. Construction of the optical fiber-based system

2.1. General concept

For the construction of an efficient detection of a bioluminescence, it is necessay to consider a collection efficiency of the luminescence at the optical fiber end and a coupling efficiency between the other optical fiber end and a photon detector as described in [4]. Using the optical fiber with a core diameter ϕ_0 and a numerical aperture NA_0, the collection efficiency of the luminescence η at the optical fiber end depends only on NA_0 as shown in Fig.3.

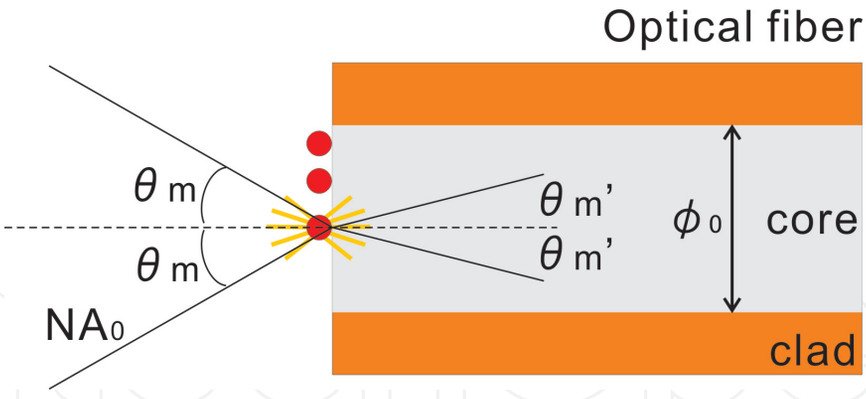

Figure 3. Luminescence at the optical fiber end. θ_m is a maximum opening angle for light propagation in the optical fiber.

From the simple calculation of the solid angle with a maximum open angle θ_m, $\eta(NA_0)$ can be expressed as,

$$\begin{aligned}\eta(NA_0) &= \frac{1}{2}(1-\cos\theta_m) \\ &= \frac{1}{2}\left[1-\sqrt{1-\left(\frac{NA_0}{n_w}\right)^2}\right],\end{aligned} \tag{1}$$

http://dx.doi.org/10.5772/52747

where n_w is the refraction index of the substance surrounding the optical fiber end. In immersing this optical fiber end into water, its value should be identical to the one of water, which is about 1.33.The caluculated values of the collection efficiency $\eta(NA_0)$ using Eq. (1) at n_w=1.33 are shown in Fig.4 as a function of NA_0. It is easy to see that $\eta(NA_0)$ monotonically increases with NA_0.

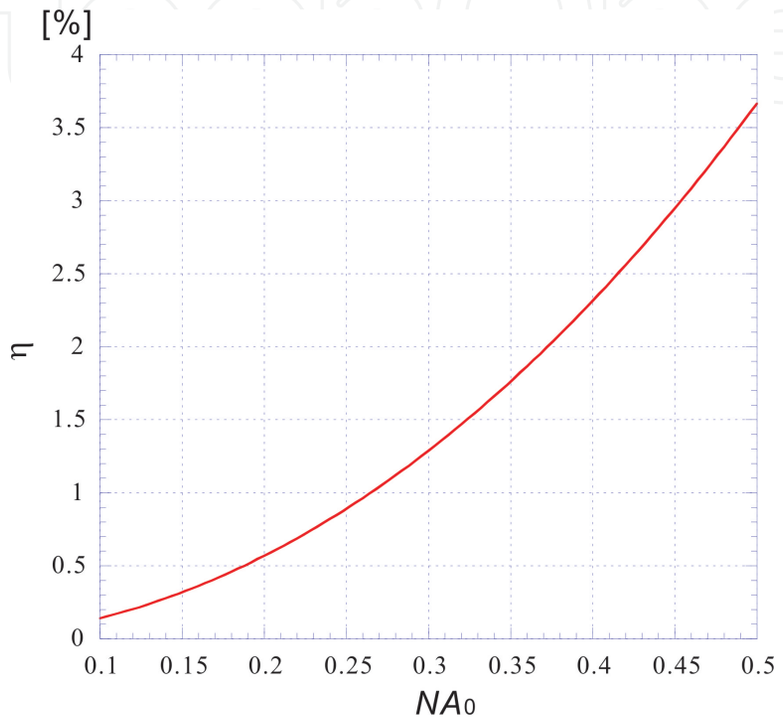

Figure 4. Calculated values of the collection efficiency η as a function of NA_0 at n_w = 1.33.

In the following, let us consider the situation where the other optical fiber end is optically coupled to a photon detector with a detection window of diameter ϕ_4 and with a circular sensitive area having a diameter ϕ_3 and a numerical aperture NA_3. The coupling efficiency ε between the optical fiber end and the photon detector depends on ϕ_0, NA_0 of the optical fiber and ϕ_3, NA_3, ϕ_4 of the photon detector used.The number of emitted photons is proportional to the square of ϕ_0 and $\eta(NA_0)$ monotonically increases with NA_0, so that the number of the transmitted photon to the other optical fiber end is proportional to ${\phi_0}^2$ and $\eta(NA_0)$. On the other hand, the coupling efficiency ε generally decreases as ϕ_0 or $\eta(NA_0)$ increases for the fixed ϕ_3, NA_3, and ϕ_4. Thus, we can define the following formula for a figure of merit (FOM) and optimize ϕ_0, NA_0 and parameters of the coupling optics x_i for the fixed values of ϕ_3, NA_3, and ϕ_4 to maximize the FOM:

$$\mathrm{FOM}={\phi}^2\cdot\eta(NA_0)\cdot\varepsilon(\phi_0,\ NA_0,\ x_i,\ \phi_3,\ NA_3,\ \phi_4) \tag{2}$$

It should be noted that the coupling efficiency ε can be ideally 100 % under the condition of $\phi_0 \leq \phi_3$ and $NA_0 \leq NA_3$.In many cases, the condition $NA_0 \leq NA_3$ is satisfied when using the typical photon detector. Under the condition $NA_0 \leq NA_3$, thus, we can categorize into two cases: case (1) is $\phi_0 \leq \phi_3$ and case (2) is $\phi_0 > \phi_3$. In the case (1), ε is constant and can be ideally 100 %, so that the detection efficiency excluding the quantum efficiency of the photon detector is only limited to $\eta(NA_0)$. Therefore, the optimization of ϕ_0 and NA_0 is not necessary. The conditions of $\phi_0 = \phi_3$ and $NA_0 = NA_3$ both maximize the FOM and the sensitivity becomes highest. In the case (2), however, the optimization of ϕ_0 and NA_0 and a specific design of the coupling optics are necessary, because the coupling efficiency ε decreases as ϕ_0 or NA_0 increases.

2.2. Construction with a cooled PMT detector

2.2.1. Photon detectors

To construct the optical fiber-based system, a choice of a single photon detector is very important. Photon detectors generally have two significant factors contributing to the sensitivity of detection for weak light: the efficiency and the dark counts of the detector. Recently, two types of single photon detectors, which are a cooled APD and a small size of cooled PMT, are available. The cooled APD which can detect for single photons is mostly used because of the high quantum efficiency and the low dark counts. The sensitive area must be very small (ϕ_0 ~0.2mm), but the quantum efficiency is several times larger than that of a typical PMT. Furthermore, it has the useful characteristics of compactness, easy operation, and durability compared to a typical PMT detector. On the other hands, the compact size of cooled PMT is also useful for the optical fiber-based system. The quantum efficiency is typically lower than the APD, but the sensitive area is roughly 10 times larger than the APD's in spite of the same dark counts as the cooled APD. Therefore, it is very easy to construct a coupling optics to the sensitive area of the detector with the high sensitivity.

We selected the PMT counting head (H7421) manufactured by Hamamatsu Photonics K.K. for this system. Its characteristics are summarized in Tab. 1. For comparison, we also present the characteristics of the APD-type photon counting module (SPCM-AQR-14) provided by Perkin Elmer. Ltd. It has already been verified that this APD is applicable to the fiber-based system by our previous investigation as discussed in [3], [4].

	Quantum efficiency (η_{qe})	**Dark noise**	**sensitive area (ϕ_3)**	**Numerical Aperture (NA_3)**	**Detection window (ϕ_4)**
PMT (H7421)	40% at 550nm	100 s^{-1}	5.0 mm	0.123	7.2 mm
APD (SPCM-AQR-14)	55% at 550nm	100 s^{-1}	0.175 mm	0.78	6.16 mm

Table 1. Characteristics of photon detectors in reference [17] and [18]

http://dx.doi.org/10.5772/52747

The value of NA_3 can be calculated from the geometrical structure between the sensitive area and the photon detection window.

2.2.2. Coupling efficiency

As showing in section 2.1, under the condition of $\phi_0 > \phi_3$, it is necessary to optimize ϕ_0, NA_0 and to design the coupling optics for maximal sensitivity. In the use of the PMT detector, it is not absolutely necessary to optimize ϕ_0, NA_0, because the characteristics of ϕ_3=5.0mm sufficiently satisfies the condition of $\phi_0 < \phi_3$ for the typical optical fiber. For easy construction, here, the optical fiber end was directly connected to the attachment of the PMT counting head without the additional coupling optics as shown in Fig. 5.

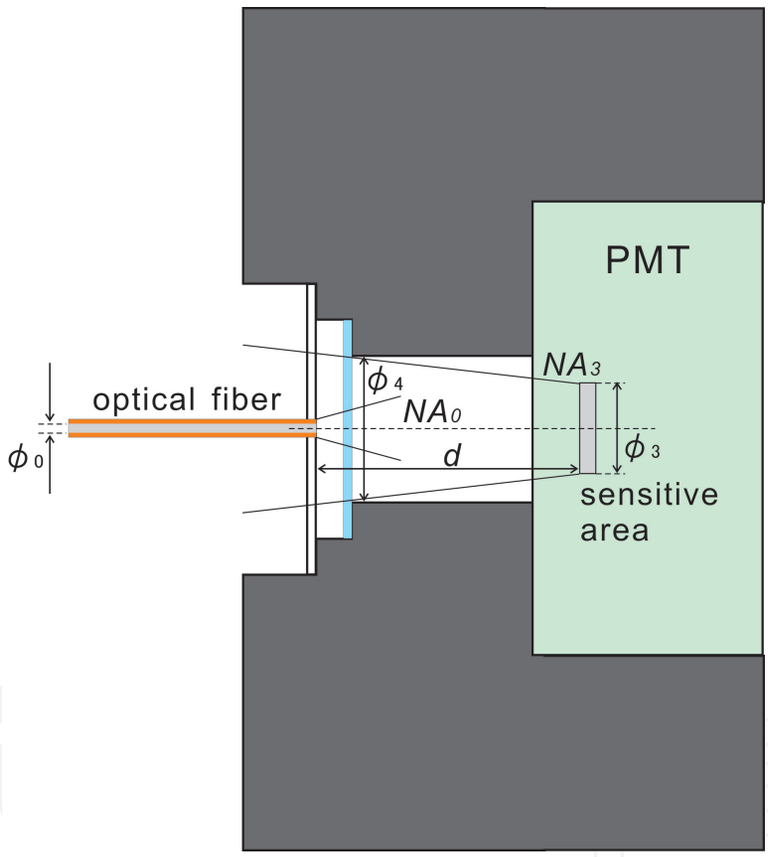

Figure 5. Geometrical structure of the PMT counting head

The coupling efficiency $\varepsilon(\phi_0, NA_0)$ in such geometrical structure can be obtained by the statistical method with matrix formalism in paraxial optics, which can describe the propagation of light. The light at the initial state (r_i, r'_i), where r_i is a distance from an optical axis and r'_i is a slope of the light direction, can be transferred by some matrices. In the case of Fig. 5, the matrix expressing free-space propagation can transfer the initial state (r_i, r'_i) at the optical fiber end to the final state (r_f, r'_f) at the PMT sensitive area. We obtained the value of

$\varepsilon(\phi_0, NA_0)$ by counting the number of the final states inside the sensitive area for many initial states selected with random numbers, which were generated by using the software package based on algorithm of Mersenne Twister in reference [19]. The calculated results are shown as a function of NA_0 in Fig. 6. Since the value of ϕ_3 is approximately 5 times as large as one of ϕ_0, the coupling efficiency $\varepsilon(\phi_0, NA_0)$ is independent of ϕ_0, but monotonically decreasing with NA_0. Therefore, we calculated the FOM for confirming the existence of optimal conditions for ϕ_0, NA_0. Fig. 7 shows the plot of the calculated FOM as a function of NA_0 and obviously indicates that the FOM is almost constant to NA_0. Thus, we determined NA_0=0.37 and ϕ_0=1.0 *mm* because of availability and flexibility of the optical fiber. These values easily give the coupling efficiency $\varepsilon(\phi_0, NA_0)$ of 21.7% and FOM×100 of 0.420.

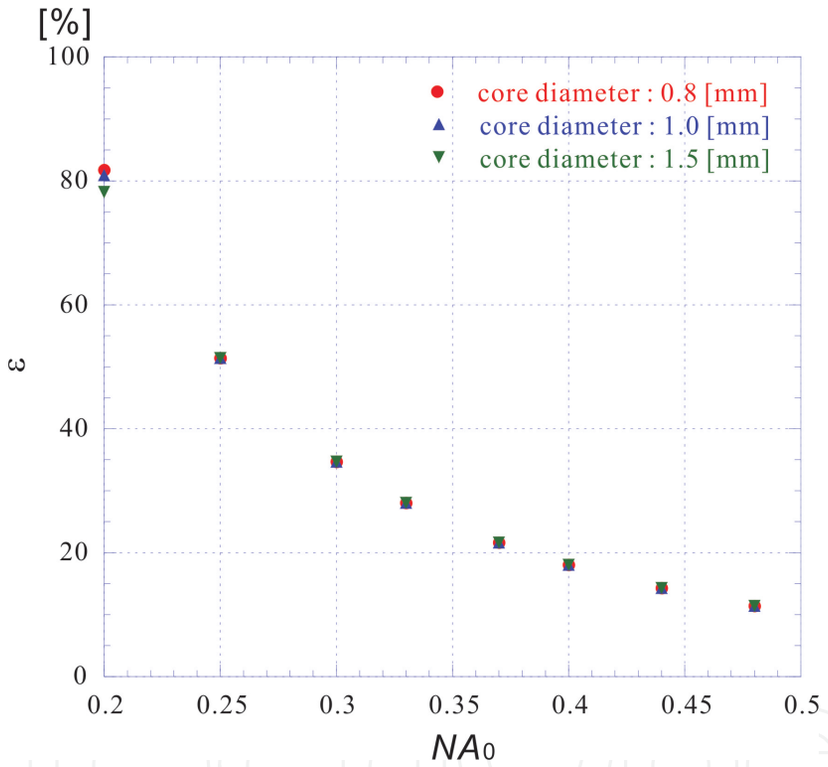

Figure 6. Calculated values of the coupling efficiency ϕ_0 as a function of NA_0. The solid circles represent the values at ϕ_0=0.8 *mm*, the solid triangles are the values at ϕ_0=1.0 *mm*, and the solid inverse triangles are the values at ϕ_0=1.5 *mm*.

On the other hands, in the use of the APD, the optimization of NA_0=0.37, ϕ_0=0.6 *mm* and the design of the optimal coupling optics are absolutely necessary. A simple optically coupling way is shown in Fig. 8. With the above APD, the condition of FOM×100 and $\varepsilon(\phi_0, NA_0)$ maximizes the FOM and the value of $\eta(NA_0)$ is 0.234. The determined design parameters of the coupling optics give the maximum ε of 33.3% and NA_0 of 1.97%. The detailed description about the determination of the design parameters is given in [3] and [4].

http://dx.doi.org/10.5772/52747

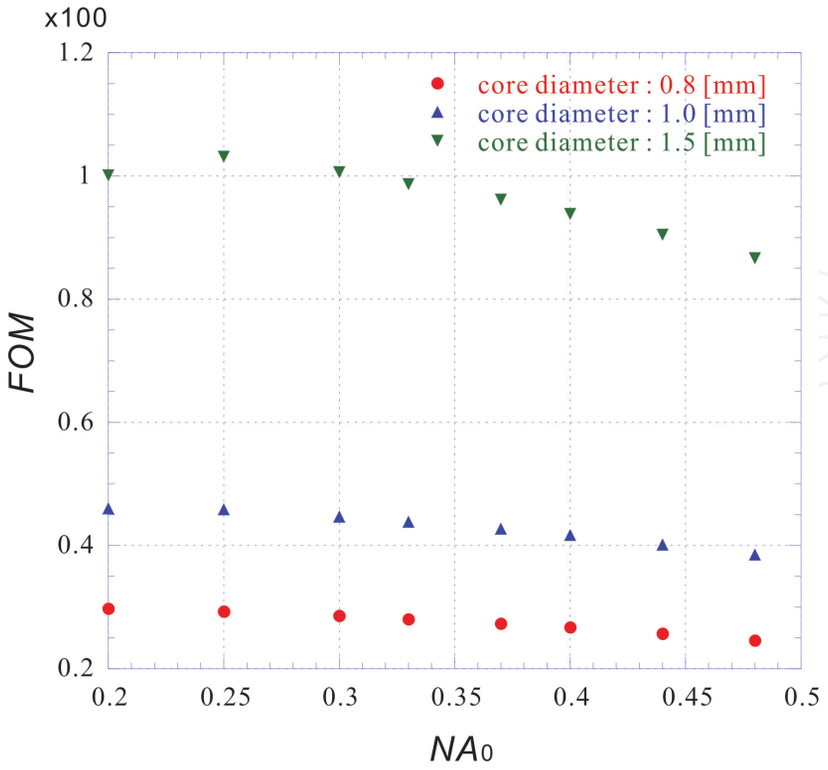

Figure 7. Calculated values of FOM as a function of NA_0. The solid circles represent the values at ϕ_0=0.8 *mm*, the solid triangles are the values at ϕ_0=1.0 *mm*, and the solid inverse triangles are the values at ϕ_0=1.5 *mm*.

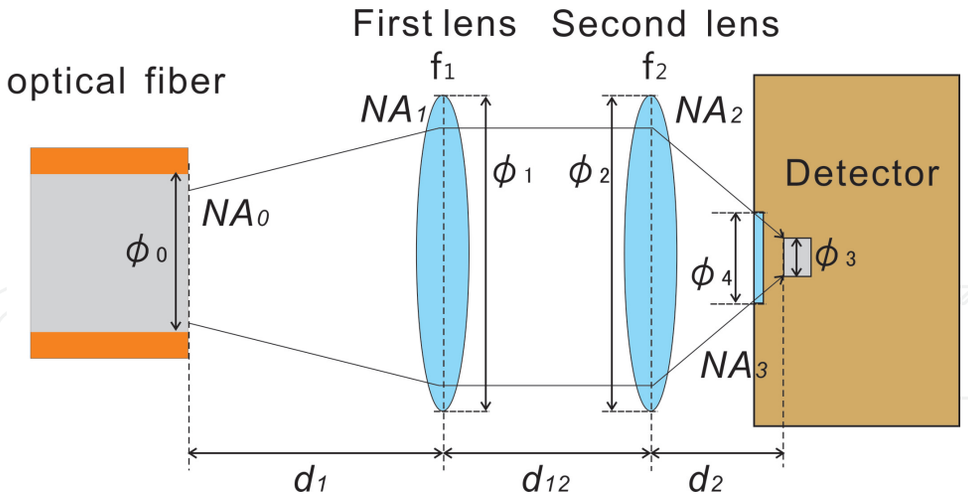

Figure 8. One example of additional coupling optics

The relative sensitivity for the bioluminescence detection can be compared by using a product of FOM and the quantum efficiency η_{qe} of the detector as an indicator. For the PMT, the value of $(\mathrm{FOM}\cdot\eta_{qe})\times 100$ is 0.168 and 0.129 for the optimal values of the above APD.In such direct connection, the sensitivity with the PMT is almost same as with the APD. For the system with

the PMT, furthermore, it should be noted that the coupling efficiency ε at NA_0=0.37 and ϕ_0=1.5 *mm* can be 100% using the additional coupling optics as shown in Fig. 8. These values give $(\mathrm{FOM} \cdot \eta_{qe}) \times 100 = 1.77$, which is about 10 times larger than the present value.

3. Sensitivity test for ATP detection

3.1. Luciferin-luciferase reaction

Bioluminescence in living organisms, such as fireflies and some marine bacteria, typically occurs due to the optical transition from the excited state to the ground state of oxidized luciferin molecules produced by the luciferin-luciferase reaction under the catalytic activity of luciferase molecules. This reaction can be expressed by the following squential of reaction steps:

$$\mathrm{E} + \mathrm{S} + \mathrm{LH_2} \rightleftarrows \mathrm{C_1} + \mathrm{PP}_i$$

$$\mathrm{C_1} + \mathrm{O_2} \rightarrow \mathrm{C_2} + \mathrm{AMP} + \mathrm{CO_2} + \gamma$$

$$\mathrm{C_2} \rightleftarrows \mathrm{E} + \mathrm{P},$$

where E indicates luciferase, S ATP, $\mathrm{LH_2}$ luciferin, PP_i pyrophoric acid, $\mathrm{C_1}$ is an enzyme-substrate compound $\mathrm{E \cdot LH_2}$-AMP, AMP adenosine monophosphate, P oxyluciferin (oxidized luciferin), $\mathrm{C_2}$ a luciferase-oxyluciferin compound, and γ a photon in reference [20]. The emission of one photon at the position of luciferase molecule corresponds to the use of the energy of one ATP molecule. Against the second reaction which is a rate-limiting reaction in the above reaction chain, it is known that the following reaction is competitive,

$$\mathrm{C_1} + \mathrm{O_2} \rightarrow \mathrm{C_3} + \mathrm{H_2O_2}$$

$$\mathrm{C_3} \rightleftarrows \mathrm{E} + \mathrm{L\text{-}AMP},$$

where L - AMP represents dehydroluciferyl-adenylate, $\mathrm{C_3}$ is an enyzme-substrate compond $\mathrm{E \cdot L}$-AMP as described in [21]. This reaction does not induce the photon emission. Dehydro-luciferyl-adenylate L - AMP as well as oxyluciferin is known as a competitive inhibitor to the equilibrium reaction in [22].

In the presence of enough luciferin molecules, the immobilization of luciferase molecules at the optical fiber end allows us to sense the present of ATP around the fiber end using single photon counts. For this purpose, we used a compound protein containing a silica-binding protein (SBP) molecule and a luciferase molecule (SBP-luciferase), which were recently synthesized by Taniguchi and co-workers in [23]. This protein makes it possible to immobilize a lucuferase molecule on the optical fiber end through a SBP molecule retaining its activity. The spectrum of the emitted photons shows a central wavelength of 550 nm and a width of about 100 nm in reference [24] and [25]. Both photon detectors of the APD and the PMT have

http://dx.doi.org/10.5772/52747

the large quantum efficiency at 550 nm, the photon counting detectors are suitable for ATP sensing.

3.2. Michaelis-Menten formula

In the solution containing nonlocalized homogeneously dispersed luciferase and ATP, the Michaelis-Menten formula is applicable to the enzyme reaction as descibed in [26]. In the presence of sufficient luciferin molecules in the solution, a rate of emitted photons at steady state v_γ can be expressed as the Michaelis-Menten formula,

$$v_\gamma = \frac{V_{max} s}{s + K_M}, \tag{3}$$

where V_{max} is a maximum reaction rate which is equivalent to a product of a concentration of luciferase molecules and a reaction constant h_1 from C_1 to C_2, K_M is the Michaelis constant, and s is the ATP concentration. In the fiber-based system for sensing dispersed ATP molecules, on the other hands, an ATP-flow generated by a gradient of ATP concentration around the luciferase-terminated fiber end carries ATP molecules to the vicinity of immobilized luciferase molecules. One of ATP molecules is bound to one immobilized luciferase molecule near them and subsequently used for the luciferin-luciferase reaction at this fiber end. By solving reaction-diffusion equations, as described in [4], we have confirmed that an ATP diffusion rate is not a rate-limiting process when the number of immobilized luciferase molecules is 10^{11} order and the ATP diffusion constant is $D = 0.5 \times 10^{-3} mm^2 / s$ given in [27]. Therefore, the Michaelis-Menten formula Eq. (3) can be also applied for the fiber-based system without change.

3.3. Mesurement of the sensitivity

3.3.1. Experimental setup

Fig.9 shows the experimental setup for the sensitvity test and the investigation of bioluminescence at the optical fiber end. One optical fiber end was optically connected to the PMT as describing in the previous section. On the other fiber end, the luciferase molecules were immobilized via SBP molecules and the bioluminescent reaction occurs by immersing the luciferase-terminated fiber end into a sample solution. The emitted photons were transmitted to the PMT through the optical fiber and TTL pulses outputted from the PMT were counted by a PC card installed in a personal computer(PC). To reducing the background light, the whole system was put into the dark box.

For the observation of the bioluminescence rising, a test tube containing the sample solution was fixed on the Z-stage, which is a motorized stage and externally controllable. By raising the test tube for immersing the luciferase-terminated fiber end after starting the data acquisition system, the photon counts rising from the background level and subsequently reaching a maximum were observed with time. The numbers of detected photons during 0.0298 s or during 0.1 s were recorded every 0.0321s or every 0.1s by the PC, respectively. These values

were obtained from a calibration test of data acquisition system. The details on the experimental setup and the measurements are described in reference [28].

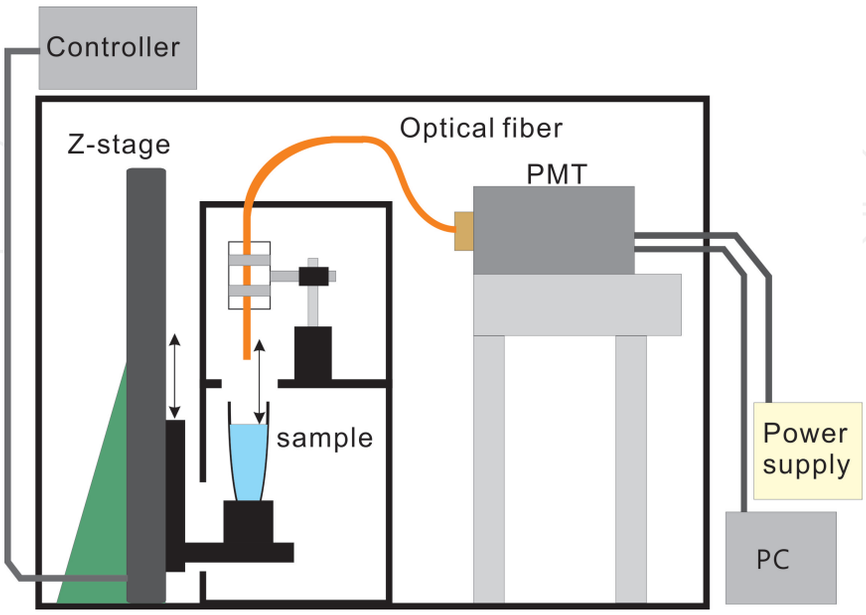

Figure 9. Experimental setup for investigation of bioluminescence at the optical fiber end

3.3.2. Immobilization of luciferase

Before immobilizing luciferase molecules, we cut the optical fiber and cleaned the cut surface with ethanol and Tris buffer (0.25mM Tris-HCl with 0.15 M NaCl). Different from the previous experiments with the APD, we cleaved the optical fiber for making a flat surface on the fiber end, which can reproduce the number of immobilized luciferase. The flat surface also allows us to indivisually evaluate the number of immobilized luciferase molecules by using element analysis, although the sensitivity with the flat surface is about 10 times lower than the one with the appropriately irregular surface cut without the cleaving technique as described in [29]. The cut surface was direcly observed by using the fiber scope and checked its flattness by eyes. After cleaning, the surface was immersed in a solultion of SBP-luciferase and was left at a temperature of 3℃ to 6℃ for a period of about two hours.

For evaluating the number of immobilized luciferase molecules, element analysis to the fiber end was carried out by using Xray Photoemission Spectroscopy (XPS). We measured a spectrum including peaks from nitrogen in the SBP-luciferase and from silicon on the surface of the fiber end which made with the silica and obtained the ratio of the area of the nitrogen-peak to the one of the silicon-peak. Utilizing the absolute number of silicon on the surface of the fiber end, the surface density of immobilized luciferase molecules was determined to be $2.0\times10^{10} mm^{-2}$. By repeating the same measurement and analysis, the error of the surface density was estimated to be 15 %.

http://dx.doi.org/10.5772/52747

3.3.3. Sample solutions

The samples were a 1:4:4:31 mixture of 20 mM D-luciferin solution, Tris buffer solution(250 mM Tris-HCl mixed with 50 mM $MgCl_2$), ATP solution, and distilled water. Several solutions of ATP with different ATP concentrations were made by diluting the ATP standard in ATP Bioluminescence Assay Kit CLS II manufactured by Roche Co. Ltd. A series of sample solutions with different ATP concentrations were prepared in advance. To obtain a background before the ATP measurements, an additional sample without ATP was also produced by mixing distilled water instead of the ATP solution.

3.3.4. Results

The time dependence of photon counts per 0.1-s interval were measured in immersing the luciferase-terminated fiber end into the sample solutions with various ATP concentration and converted to the values of photon counting rate. A typical result for 100 μl at the ATP concentration of 1.65×10^{-6} M is shown in Fig. 10.

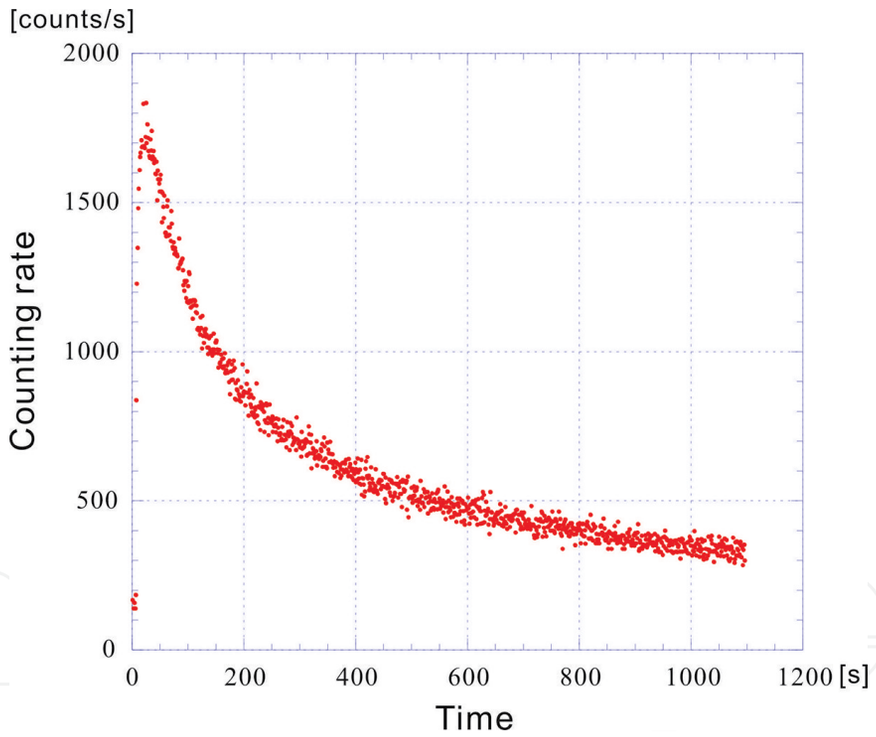

Figure 10. Time dependence of measured counting rate for 100 μl at the ATP concentration of 1.65×10^{-6} M.

The photon counts rise up, reach a maximum at about 100 s, and decrease toward the background level with time scale of 1000 s after the immersion. The background level was about 130 s^{-1}, which was essentially determined by the dark counts. For observing the detection limit of the ATP concentration, we obtained the integrated counts of detected photons over the time range from 0 to 100 s for various ATP concentrations. The result is shown as a function of the ATP concentration in Fig. 11.

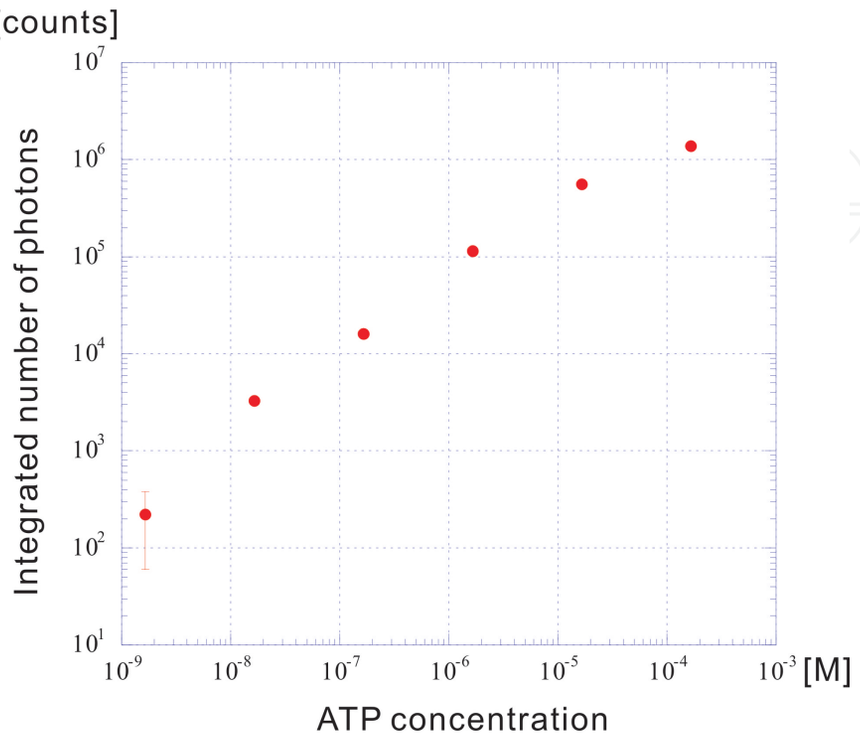

Figure 11. Number of photons integrated over the time range from 0 to 100 s as a function of ATP concentration.

Statistical errors were estimated as one standard deviation assuming Poisson distribution. From Fig. 11, the sensitivity in this system is limited to 1.65×10^{-9} M, whichcorresponds to a number of ATP molecules of about 10^{-14} mol in the 10 μl solution. This value is about 10 times higher than the one in the previous experiment with the APD as described in [3] and [4], although the FOM of this system is almost same as of the APD system. In this experiment, the surface flatness of the luciferase-terminated fiber end makes us identify the effective area as the cross section of the cut surface, as while the effective area of the cut surface in the previous experiment with the APD system was enlarged due to a surface asperity.On the effect of such different cutting ways, we have already confirmed that the sensitivity in the flat surface is about 10 times lower than the one in the appropriately irregular surface cut without the cleaving technique. Therefore, the above results are consistent with our previous results by using the APD.

To check the ATP concentration dependence of the photon counting rate at maximum, the average of counts in sixteen 1-s intervals around the time at which the counting rate become maximal was calculated for each ATP concentration. The results are indicated by the solid circles in Fig. 12. By the analysis of fitting data points in Fig. 12 to Eq. (3), we obtained the Michaelis constant of $K_M = 6.47\times10^{-5}$ M and the maximum reaction rate of $V_{max} = 7.38\times10^{4} s^{-1}$.

http://dx.doi.org/10.5772/52747

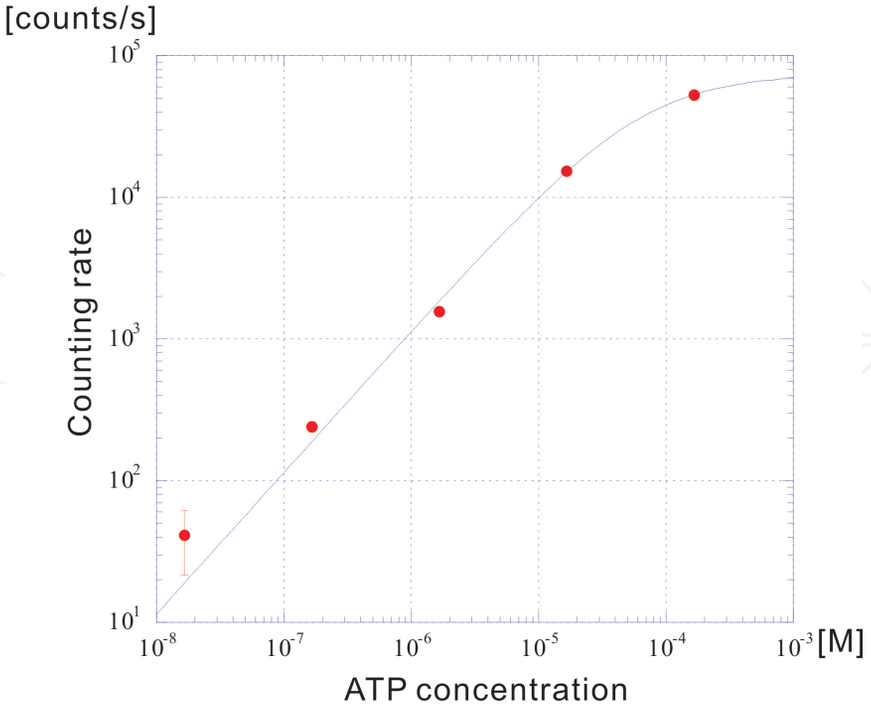

Figure 12. Measured photon counting rate as a function of ATP concentrations. Solid line is a curve obtained by fitting data with the Michaelis-Menten formula.

3.3.5. Discussion

The detection limitis essentially determined by both of the parameter V_{max} and the dark noise of the photon detector. Since the V_{max} can be expressed as $V_{\max}=\varepsilon_{total}\cdot h_1\cdot e_0$, where h_1 is a reaction rate of one luciferase molecule, e_0 is a total number of immobilized luciferase molecules on the optical fiber end and ε_{total} is a total detection efficiency, we can calculate the value of V_{max} with $\varepsilon_{total}=\eta\cdot\varepsilon\cdot\eta_{qe}$ which is 0.00171 at 550 nm, ϕ_0=1 mm, the surface density of immobilized luciferase given by $2.0\times10^{10}mm^{-2}$, and h_1=0.125 s^{-1} in reference [30]. The prediction of V_{max} is $3.36\times10^{6}s^{-1}$, which is two orders of magnitude larger than the obtained value of $7.38\times10^{4}s^{-1}$. In our previous experiment with the APD, the predicted value of V_{max} was also one order of magnitude rather than the obtained one. Possible reasons are a reduction of h_1, or an existance of inactive luciferase molecules, or both of them as discussed in reference [4] and [31]. To clarify the reason, it is necessary to individually evaluate the number of active immobilized luciferase molecules e_a and the reaction rate h_1, respectively, from experimental data.

In the PMT system, it is noted that the improvement of two orders of magnitude for V_{max} is promising by using the optimal optics coupled to the optical fiber with ϕ_0=1.5 mm and NA_0=0.37 and the optical fiber end with the appropriately irregular surface cut without the cleaving technique for immobilizing the luciferase.

4. Investigation of bioluminescence at the optical fiber end

4.1. Measurement of the bioluminescence with high time resolution

To obtain the reaction rate h_1, the number of acitve luciferase molecules e_a, and other kinetic parameters from experimental data, the counts of photons with high time resolution and the advaced analysis to such data are necessary. The data acquisition system has a capability of recoding the numbers of detected photons every 0.0321s. By making a full use of this specification, the time dependence of detected photons with high time-resolution at the ATP concentration of 1.65×10^{-4} M was obtained as shown in Fig. 13.

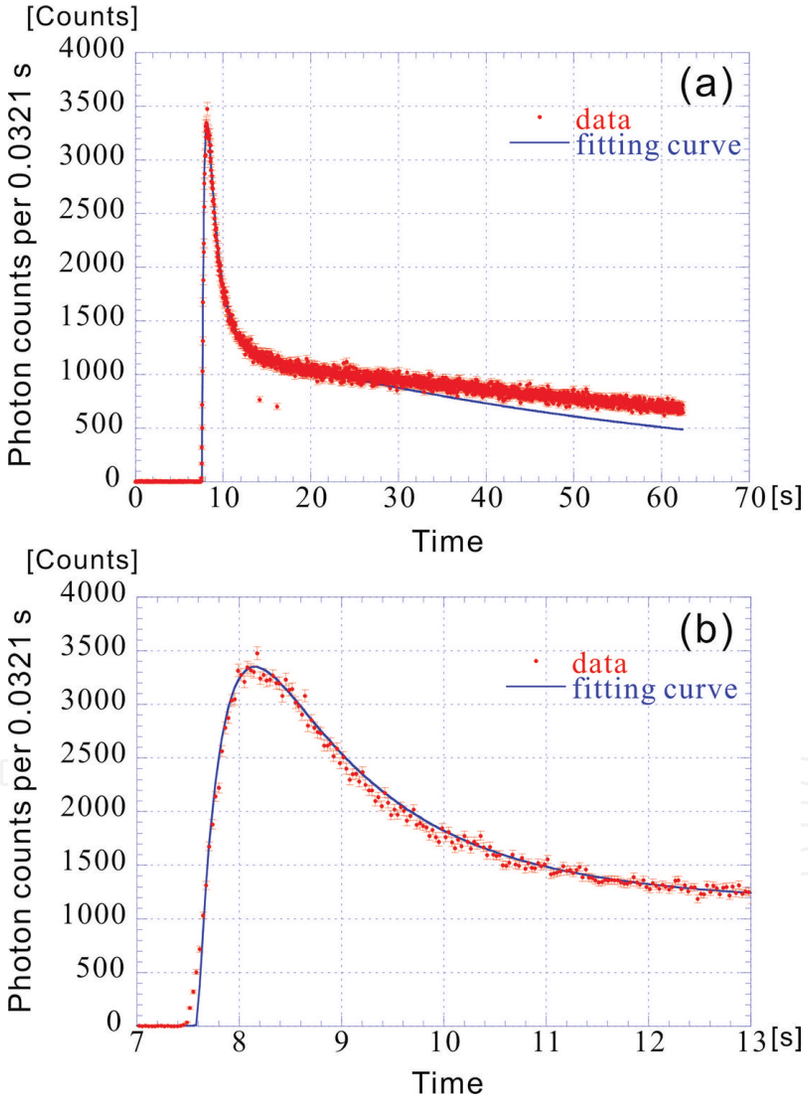

Figure 13. Time dependence of detected photons with the resolution of 0.0312 s at the ATP concentration of 1.65×10^{-4} M. The upper figure (a) shows the result in the solution of 100 μl. Solid line represents an extrapolation of the fitting curve with the parameters obtained by fitting the data from 0 s to 30 s. The lower figure (b) shows a magnified plot around the peak.

http://dx.doi.org/10.5772/52747

Fig. 13 (a) shows the result of the detected photons with the immobilized SBP-luciferase molecules at the optical fiber end into the solution of 100 μl at the ATP concentration of 1.65×10^{-4} M. For comparison, we also measured the time depencence of the photons with homogeniously dispersed SBP-luciferase molecules in the solution of 500 μl. The direct measurement of bioluminescence was carried out with an other type of cooled PMT detector having a huge sensitve area of 1 cm × 1 cm to detect the bioluminescence from a large area of the solution. The details on the direct measurement and the data analysis for dispersed luciferase molecules are given in reference [28].

4.2. Analysis

4.2.1. Reaction model including inhibitors

For obtaining kinetic parameters of bioluminescient reaction, we consider the rate equations including the effects of inhibitors. In the luciferin-luciferase reaction, two kinds of products, oxyluciferin and L - AMP are strong cometitive inhibitors to substrates. Each equilibrium constant for exyluciferin K_i and for L - AMP K_j has been measured and the values of $K_i = 0.5\ \mu M$ and $K_j = 3.8$ nM are given in reference [22]. For simplicity of the model, we assume that two inhibitors contribute the competitive inhibition to the equilibrium reactions between luciferase and ATP in the presence of enough luciferin molecules. Fig. 14 shows the reaction steps of luciferin-luciferase reaction including the effects of competitive inhibitors.

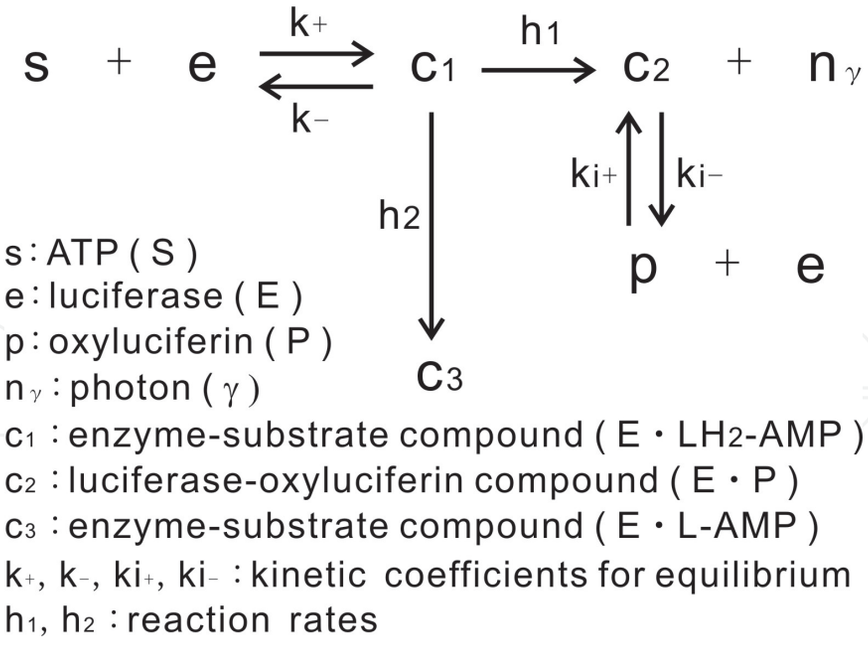

Figure 14. Enzyme reaction including the inhibitors

Here, s, e, p, n_γ, c_1, c_2, c_3 in Fig. 14 represents a concentration of ATP, luciferase, oxyluciferin, photon, E · LH_2-AMP, E · P, and E · L-AMP, respectively, k_+, k_-, k_{i+}, and k_{i-} are kinetic coeffi-

cients for equilibrium and h_1 and h_2 are reaction rates. Since the inhibition by L - AMP is much stronger than the ones by oxyluciferin, it can be assumed that the enzymes in the state of the enzyme-susbstrate compound do not release L - AMP molecules and concequently lose the activation in the time scale of our experiment.

In the use of the immobilized luciferase molecules for sensing dispersed ATP molecules, it is natural to consider that the reaction occures in a volume ΔV which is the vicinity of the luciferase-terminated optical fiber end. Therefore, the serise of the rate equations describing the enzyme reaction shown in Fig. 14 in the volume ΔV can be expressed as

$$\frac{de}{dt} = - k_+ es + k_- c_1 + k_{i-} c_2 + k_{i+} ep \tag{4}$$

$$\frac{dc_1}{dt} = k_+ es - \left(k_- + h_1 + h_2\right) c_1 \tag{5}$$

$$\frac{dc_2}{dt} = h_1 c_1 - k_{i-} c_2 + k_{i+} ep \tag{6}$$

$$\frac{dc_3}{dt} = h_2 c_1 \tag{7}$$

$$\frac{dn_\gamma}{dt} = h_1 c_1 \tag{8}$$

$$\mathrm{N}_A V_0 \frac{ds}{dt} = - k_+ se + k_- c_1 \tag{9}$$

$$\mathrm{N}_A \Delta V \frac{dp}{dt} = - k_{i+} ep + k_{i-} c_2, \tag{10}$$

where the variable e, n_γ, c_1, c_2, c_3 is a number of each kind of molecules or photon in the volume ΔV. The variable s and p is the concentration of ATP and oxyluciferin, respectively, and their unit is M. The N_A is Avogadro number and the V_0 is a volume of the solution. The unit of k_-, k_{i-}, h_1, h_2 is s^{-1} and of k_+, k_{i+} is $\mathrm{M}^{-1}s^{-1}$. The volume V_0 is explicitly utilized into Eq. (9), since the concentration of ATP in the volume of V_0 is almost same as in the volume of ΔV because of a rapid diffusion rate. The volume ΔV can be approximately considered as a cylinder with a diameter of ϕ_0 =1 mm and a height of 10 nm because the size of SBP-luciferase molecules is about several nanometer, and its value is $\Delta V = 7.85 \times 10^{-12}$ l.

In addition to the above rate equations, the following conditions described as,

$$e_a = e + c_1 + c_2 + c_3 \tag{11}$$

$$n_\gamma = c_2 + \mathrm{N}_A \Delta V p \tag{12}$$

http://dx.doi.org/10.5772/52747

should be satisfied. The condition of Eq. (11) shows that the total number of active luciferase molecules e_a is constant and Eq. (12) means that the total number of photons is equivalent to that of oxyluciferin molecules. The Michaelis constant K_m and the equilibrium constant of oxyluciferin K_i can be expressed as

$$K_m = (k_- + h_1 + h_2)/k_+ \tag{13}$$

$$K_i = k_{i-}/k_{i+} \tag{14}$$

Using Eq. (11), Eq. (12), Eq. (13), and Eq. (14) as boundary conditions and inputting the constant values of e_a, h_1, h_2, k_+, k_{i-}, K_m, K_i and the initial values for variables, we can numerically solve the rate equations and obtain the time evolution of n_γ as the numerical solution at each time step. To simplify the numerical calculation, we assumed that oxyluciferin molecules instantaneously move out from the volume of ΔV because of the fast diffusion rate of the oxyluciferin molecules. Therefore, the kinetic constant k_{i+} can be practically zero. This treatment means that the influence of the competitive inhibition by the oxyluciferin can be neglected.

In the solution containing non-localized homogenous dispersed SBP-luciferase, the volume of ΔV in the equations is replaced with the volume of the solution V_0 and the kinetic constant k_{i+} is treated as non-zero.

4.2.2. Results of analysis

The five parameters $\mathbf{a}(e_a, k_+, k_{i-}, h_1, h_2)$ were treated as fitting parameters and the data was fitted to numerical solution of n_γ for obtaining the values of **a**. As the first step, by inputting the initial values of **a** to the rate equations, the emitted photon $N_{th}^i(\mathbf{a})$ was calculated every time step of 0.0321 s with $K_i = 0.5\ \mu$M given in [22] and $K_m = 6.47 \times 10^{-5}$ M, which was deduced from the data analysis shown in Fig. 12. The data-set of $N_{th}^i(\mathbf{a})$, the n_0 number of measurend counts per 0.0321 s N_{exp}^i, and the background counts N_{exp}^0 enable us to calculate a chi-square χ^2 with the formula given by

$$\chi^2(\mathbf{a}) = \sum_{i=1}^{n_0} \frac{\{(N_{exp}^i - N_{exp}^0) - N_{th}^i(\mathbf{a})\}^2}{(N_{exp}^i + N_{exp}^0)} \tag{15}$$

The chi-square $\chi^2(\mathbf{a})$ is a good indicator for fitting data and its minimum gives the optimal combination of probable values in **a**. Solving the series of the rate equations was executed by using the software package RKSUITE based on the Runge-Kutta method [32] and the minimization of the chi-square was performed with routines of MINUIT package provided by CERN software [33].

The result of fitting the data from 0 s to 30 s is represented as a solid line in Fig. 13 (a), which is extrapolated to 60 s using the obtaind parameters. This result is not reproduced completely in the time range from 0 s to 60 s, because the effect of the competitive inhibition of oxyluciferin is not considered and the fitting fuction includes only the contribution of the deactivation process. The inhibition of the oxyluciferin weakens with time due to its diffusion process, but this diffusion effect is not considered in this analysis. In contrast, the contribution of the deactivation process, which was evaluated by fitting the data around the peak, is concequently overestimated compared to the actual contribution. Therefore, the effect of the relatively strong evaluation for the deactivation process appears in the time range after 30 s.

The parameters obtained by fitting the data are summarized in table 2 together with the results of the dispersed luciferase for comparison. The parameter r represents the activation ratio of the SBP-luciferase, which can be defined as a ratio of the number of active luciferase molecules e_a to the total number of immobilized luciferase molecules e_0, which can be calculatedfrom the surface density of immobilized SBP-luciferase or from the concentration of the dispersed SBP-luciferase. In addtion, the parameter k_- and k_{i+} was derived from Eq. (13) and Eq. (14), respectively. The statistical error was 3 % at the maximum, but the systematical error was estimated to be 20 % taking account of the errors of the numerical calculation and the parameters used.

	dispersed luciferase	**immobilized luciferase**
Volume of solution	**500 µl**	**100 µl**
Region used for fitting	**0 – 60 s**	**0 – 30 s**
$r\ (e_a / e_0)$	0.44	0.010
k_+	$1.7\times10^4 M^{-1}s^{-1}$	$2.1\times10^4 M^{-1}s^{-1}$
h_1	$0.21s^{-1}$	$0.61s^{-1}$
h_2	$0.090s^{-1}$	$0.073s^{-1}$
k_{i-}	$0.090s^{-1}$	$0.25s^{-1}$
k_-	$0.83s^{-1}$	$0.68s^{-1}$
k_{i+}	1.8×10^5	

Table 2. Summary of obtained parameters

4.3. Discussion

In table 2, it is easily seen that the kinetic parameters in the immobilized luciferase are almost same as in the non-localized dispersed luciferase except the reaction rate of h_1. Since the rising time is approximately given by $1/k_+s$, it is useful for checking a consistency of k_+ with the reference. For dispersed luciferase, the rising time of 0.29 s is obtained with $k_+=1.7\times10^4 M^{-1}s^{-1}$ and for immobilized luciferase, the rising time of 0.36 s is given by the value of

http://dx.doi.org/10.5772/52747

k_+=2.1×10^{4}M^{-1}s^{-1}. Both of them are close to the value of 0.3 s in reference [34], so that their values are consistent with the reference.

On the reaction rates, the obtained value of h_1=0.61 s^{-1} for immobilized lucifrase is about 5 times larger than the reference value 0.125s^{-1} given in [30], but the order of both values is the same. A more precise comparison is not meaningful, because the surrounding environment of luciferase is not exactly same as in the reference.On the other hands, a branching ratio to the deactivation process, which is given by $h_2/(h_1+h_2)$, can be estimated to be 30 % for immobilized luciferase and 10 % for dispersed luciferase, respectively. Since the reference value of 20 % is given in [22], both of them are close to the refrence value. Thus, we can consider the obtained values of the parameters are almost consistent with the values which had been measured so far.

From table 2, the activation ratio r is 44 % for the dispersed SBP-luciferase and 1 % for the immobilized SBP-luciferase, respectively. In contrast, the reaction rate h_1 is the same order as the value we expected. Therefore, the detection limit for ATP detection results in two orders of magnitude larger than the expected one. As a concequence, the results of the sensitivity test described in Section 3 can be explained from the reduction of the activation ratio for the immobilized luciferase molecules.

5. Summary

We introduced a method of high-sensitivity detection of bioluminescence at an optical fiber end for an ATP detection as an efficient alternative to direct detection of bioluminescence for a sample solution. For investigation of the bioluminescence, we constructed an optical fiber-based system, where the luciferase molecules are immobilized on the optical fiber end and the other end is optically coupled to a compact size of cooled PMT-type photon counting head which has a large sensitive area. Although the sensitivity for the bioluminescence is not optimal, it is almost same as the system which had been constructed with an APD-type photon counting detector. We have evaluated the sensitivity for ATP detection and verified the detection limit of 10^{-9} M which is consistent with the previous results with the APD-type detector. This detector limit allows us to detect the absolute ATP number of 10^{-14} mol in a 10 μl solution, but it is two orders of magnitude larger than the expected one. For clarifying the reason, we have performed measurements with high time resolution and analyses of data by using an enzyme reaction model including inhibitors to individulally obtain an activation ratio and a reaction rate of the immobilied luciferase. As the results, the reaction rate of 0.61 s^{-1} and the activation ratio of 1 % have been obtained and these results have explained the reason of two orders of magnitude higher than the expected one. For reducing the detection limit more, it is necessary to improve the activtion ratio of the immobilized luciferase on the optical fiber end as well as the enlargement of the effective area of the cut surface based on a surface asperity and the increase of the FOM with the optimal values of a core diameter ϕ_0, a numerical aperture NA_0 and parameters of the coupling optics.

Acknowledgements

We are grateful to Prof. Hiroyuki Sakaue for supporting the element analysis with XPS and Prof. Kenichi Noda for useful supports to the experiments. This work has been partially supported by the International Project Center for Integration Research on Quantum, Information, and Life Science of Hiroshima University and the Grant-in-Aid for Scientific Research (C) (19560046) of Japanese Society for the Promotion of Science, JSPS.

Author details

Masataka Iinuma, Ryuta Tanaka, Eriko Takahama, Takeshi Ikeda, Yutaka Kadoya and Akio Kuroda

Graduate School of Advanced Sciences of Matters, Hiroshima University, Japan

References

[1] Arnold M. A. Fluorophore- and Chromophore-Based Fiberoptic Biosensors. In: Blum L. J. and Coulet P. R. (ed.)Biosensor principles and applications. New York: Marcel Dekker; (1991), 195-211.

[2] Blum L. J. and Gautier S. M.Bioluminescence- and Chemiluminescence-Based Fiberoptic Sensors. In: Blum L. J. and Coulet P. R. (ed.)Biosensor principles and applications. New York: Marcel Dekker; (1991), 213-247.

[3] Iinuma M., Ushio Y., Kuroda A., Kadoya Y.High Sensitivity Detection of ATP Using Bioluminescence at An Optical Fiber End. Electronics and Communications in Japan (2009), 92(9), 53-59. Available from http://onlinelibrary.wiley.com/doi/10.1002/ecj.10054/abstract (accessed 20 August 2009).

[4] Iinuma M., Ushio Y., Kuroda A., Kadoya Y. High-Sensitivity Detection of Bioluminescence at an Optical Fiber End for an ATP Sensor. In: Yasin M., Harun S. W., Arof H. (ed.) Fiber Optic Sensor. Rijeka; InTech; (2012), 459-474. Available from http://www.intechopen.com/books/fiber-optic-sensor (accessed 22 February 2012).

[5] Stanley P. E.A survey of more than 90 Commercially Available Luminometers and Imaging Devices for Low-light Measurements of Chemiluminescence and Bioluminescence, Including Instruments for Manual, Automatic and Specialized Operation, for HPLC, LC, GLC and Microtitre Plates. Journal of Bioluminescence and Chemiluminescence (1992), 7(2), 77-108. Available from http://onlinelibrary.wiley.com/doi/10.1002/bio.1170070202/abstract (accessed 30 March 2005).

[6] Andreotti P. E., Berthold F. Application of a new high sensitivity luminometer for industrial microbilogy and molecular biology. Luminescence (1999), 14(1), 19-22. Avail-

able from http://onlinelibrary.wiley.com/doi/10.1002/%28SICI%291522-7243%28199901/02%2914:1%3C19::AID-BIO512%3E3.0.CO;2-8/abstract (accessed 26 March 1999).

[7] Gourine A. V., Laudet E., Dale N.,Spyer K. MATP is a mediator of chemosensory transduction in the central nervous system. Nature (2005), 436, 108-111. Available from http://www.nature.com/nature/journal/n7047/full/nature03690.html (accessed 25 April 2005).

[8] Fraga H. Firefly luminescence: A histrical perspective and recent developments. Photochemical and Photobiological Sciences (2008), 7(2):146-158. Available from http://pubs.rsc.org/en/content/articlepdf/2008/pp/b719181b (accessed 23 January 2008).

[9] Nakamura M., Mie M., Funabashi H., Yamamoto K., Ando J, Kobatake E.Cell-surface-localized ATP detection with immobilized firefly luciferase. Analytical Biochemistry (2006), 352(1), 61-67. Available from http://www.sciencedirect.com/science/article/pii/S0003269706001394 (accessed 19 February 2006).

[10] Konno T., Ito T., Takai M., Ishihara K.Enzymatic photochemical sensing using luciferase-immobilized polymer nanoparticles covered with artificial cell membrane. Journal of Biomaterials Sciences, Polymer Edition (2006), 17(12), 1347-1357. Available from http://www.tandfonline.com/doi/abs/10.1163/156856206778937235 (accessed 2 April 2012).

[11] Lee Y., Jablonski I., DeLuca M. Immobilization of Firefly Luciferase on Glass Rods: Properties of the Immobilized Enzyme. Analytical Biochemistry (1977), 80(2), 496-501. Available from http://www.sciencedirect.com/science/article/pii/0003269777906728 (accessed 7 December 2004).

[12] Blum L. J., Coulet P. R., Gautheron D. C.Collagen Strip with Immobilized Luciferase for ATP Bioluminescent Determination. Biotechnology and Bioengineering (1985), 27(3), 232-237. Available from http://onlinelibrary.wiley.com/doi/10.1002/bit.260270304/abstract (accessed 18 February 2004).

[13] Ribeiro A. R., Santos R. M., Rosario L. M., Gil M. H.Immobilization of Luciferase from a Firefly Lantern Extract on Glass Strips as an Alternative Strategy for Luminescent Detection of ATP. Journal of Bioluminescence and Chemiluminescence (1998), 13(6), 371-378. Available from http://onlinelibrary.wiley.com/doi/10.1002/%28SICI%291099-1271%28199811/12%2913:6%3C371::AID-BIO510%3E3.0.CO;2-%23/abstract (accessed 13 January 1999).

[14] Worsfold P. J., Nabi A.Bioluminescent assays with immobilized firefly luciferase based on flow injection analysis. Analytica Chimica Acta (1986), 179, 307-313. Available from http://www.sciencedirect.com/science/article/pii/S000326700084475X (accessed 4 January 2002).

[15] Tanii T., Goto T., Iida T., Koh-Masahara M., Ohdomari I. Fabrication of Adenosine Triphosphate-Molecule Recognition Chip by Means of Bioluminous Enzyme Lucifer-

ase. Japanese Journal of Applied Physics (2001), 40, L1135-L1137. Available from http://jjap.jsap.jp/link?JJAP/40/L1135/ (accessed 24 August 2001).

[16] Tsuboi Y., Furuhata Y., Kitamura N. A sensor for adenosine triphosphate fabricated by laser-induced forward transfer of luciferase onto a poly(dimethylsiloxane) microchip. Applied Surface Science (2007), 253, 8422-8427. Available from http://www.sciencedirect.com/science/article/pii/S0169433207005399 (accessed 13 April 2007).

[17] Hamamatsu Photonics K. K. Manual on H7421 series photon counting head.

[18] Perkin Elmer. Ltd. datasheet of SPCM-AQR-14%2F15%2F16-datasheet.html (accessed 2012).

[19] Matsumoto M., Nishimura T.Mersenne Twister: A 623-dimensionally equidistributed uniform pseudorandom number generator. ACM Transaction modellingand computer simulation (1998), 8, 3-30. Available from http://dl.acm.org/citation.cfm?id=272995&CFID=226399843&CFTOKEN=43874926 (accessed 1 January 1998). l

[20] DeLuca M.Firefly luciferase. In: Meister A. (ed.)Advances in Enzymology. New York; Wiley; (1976), 44, 37-68.

[21] Fraga H., Fernandes D., Novotny J., Fontes R., Esteves da Silva J. C. G. Firefly Luciferase Produces Hydrogen Peroxide as a Coproduct in Dehydroluciferyl Adenylate. ChemBioChem (2006), 7(6), 929-935. Available from http://onlinelibrary.wiley.com/doi/10.1002/cbic.200500443/abstract (accessed 27 April 2006).

[22] Ribeiro C., Esteves da Silva J. C. G. Kinetics of inhibition of firefly luciferase by oxyluciferin and dehydroluciferyl-adenylate. Photochemical and Photobiological Sciences (2008), 7(9), 1085-1090. Available from http://pubs.rsc.org/en/content/articlelanding/2008/pp/b809935a (accessed 1 August 2008).

[23] Taniguchi K., Nomura K., Hata Y., Nishimura Y., Asami Y., Kuroda A. The Si-tag for immobilizing proteins on a silica surface. Biotechnology and Bioengineering (2007), 96(6), 1023-1029. Available from http://onlinelibrary.wiley.com/doi/10.1002/bit.21208/abstract (accessed 29 September 2006).

[24] Denburg J. L., Lee R. T., McElory W. DSubstrate-Binding Properties of Firefly Luciferase 1. Luciferin-binding Site. Archives of Biochemistry and Biophysics (1969), 134(2), 381-394. Available from http://www.sciencedirect.com/science/article/pii/0003986169902975 (accessed 26 October 2004).

[25] Ugarova N. N., Brovko L. Y. Protein structure and bioluminescent spectra for firefly bioluminescence. Luminescence (2002), 17(5), 321-330. Available from http://onlinelibrary.wiley.com/doi/10.1002/bio.688/abstract (accessed 23 September 2002).

[26] Silbery R. J., Alberty R. A., Bawendi M. G. Physical Chemistry 4h edition. Wiley;2004.

[27] Aflao C., DeLuca M.Continuous Monitoring of Adenosine 5'-Triphosphate in the Microenvironment of Immobilized Enzymes by Firefly Luciferase. Biochemistry (1987), 26(13), 3913-3920. Available from http://pubs.acs.org/doi/abs/10.1021/bi00387a026

[28] Tanaka. R., Takahama E., Iinuma M., Ikeda T., Kadoya Y., Kuroda A. Bioluminescent Reaction by Immobilized Luciferase. IEEJ Transactions on Electronics, Information and Systems (2011), 131(1), 23-28. Available from https://www.jstage.jst.go.jp/article/ieejeiss/131/1/131_1_23/_article (accessed 1 January 2011)

[29] Ushio Y. Improvement of the sensitivity for ATP detection by the efficient optical coupling between a biosensor and an APD-type of photon detector. Master thesis. Hiroshima University Higashi-Hiroshima; 2007.

[30] Branchini B. R., Magyar R. A., Murtiashaw M. H., Portier N. CThe Role of Active Site Residue Arginie 218 in Firefly Luciferase Bioluminescence. Biochemistry (2001), 40(8), 2410-2418. Available from http://pubs.acs.org/doi/abs/10.1021/bi002246m (accessed 1 January 2001)

[31] Nishiyama K., Watanabe T., Hoshina T., Ohdomari I.The main factor of the decrease in activity of luciferase on the Si surface. Chemical Physics Letters (2008), 453(4-6), 279-282. Available from http://www.sciencedirect.com/science/article/pii/S0009261408000882 (accessed 21 January 2008).

[32] Netlib Repository Library rksuite. http://www.netlib.org/ode/rksuite/

[33] Minuit home page. http://seal.web.cern.ch/seal/work-packages/mathlibs/minuit/home.html/

[34] DeLuca M., McElory W. D.Kinetics of the Firefly Luciferase Catalyzed Reactions. Biochemistry (1974), 13(5), 921-925. Available from http://pubs.acs.org/doi/abs/10.1021/bi00702a015

IntechOpen